Cation Effects on Interfacial Water Organization of Aqueous Chloride Solutions. I. Monovalent Cations: Li+, Na+, K+, and NH4+

ARTICLE *in* THE JOURNAL OF PHYSICAL CHEMISTRY B · MAY 2014

Impact Factor: 3.3 · DOI: 10.1021/jp503132m · Source: PubMed

5 AUTHORS, INCLUDING:

Wei Hua
The Ohio State University
24 PUBLICATIONS **501** CITATIONS
SEE PROFILE

Dominique Verreault
The Ohio State University
24 PUBLICATIONS **137** CITATIONS
SEE PROFILE

Ellen M Adams
The Ohio State University
9 PUBLICATIONS **33** CITATIONS
SEE PROFILE

Heather C Allen
The Ohio State University
126 PUBLICATIONS **3,389** CITATIONS
SEE PROFILE

THE JOURNAL OF PHYSICAL CHEMISTRY B

Article

pubs.acs.org/JPCB

Cation Effects on Interfacial Water Organization of Aqueous Chloride Solutions. I. Monovalent Cations: Li^+, Na^+, K^+, and NH_4^+

Wei Hua, Dominique Verreault, Zishuai Huang, Ellen M. Adams, and Heather C. Allen*

Department of Chemistry & Biochemistry, The Ohio State University, 100 West 18th Avenue, Columbus, Ohio 43210, United States

Supporting Information

ABSTRACT: The influence of monovalent cations on the interfacial water organization of alkali (LiCl, NaCl, and KCl) and ammonium chloride (NH_4Cl) salt solutions was investigated using surface-sensitive conventional vibrational sum frequency generation (VSFG) and heterodyne-detected (HD-)VSFG spectroscopy. It was found in the conventional VSFG spectra that LiCl and NH_4Cl significantly perturb water's hydrogen-bonding network. In contrast, NaCl and KCl had little effect on the interfacial water structure and exhibited weak concentration dependency. The Im $\chi_s^{(2)}(\omega_{IR})$ spectra from HD-VSFG further revealed that, for all chloride solutions, the net transition dipole moments of hydrogen-bonded water molecules (O → H) are oriented more toward the vapor phase relative to neat water. This suggests the presence of an interfacial electric field generated from the formation of an ionic double layer in the interfacial region with a distribution of Cl^- ions located above the countercations, in agreement with predictions from MD simulations. The magnitude of this electric field shows a small but definite cation specificity and follows the order $Li^+ \approx Na^+ > NH_4^+ > K^+$. The observed trend was found to be in good agreement with previously published surface potential data.

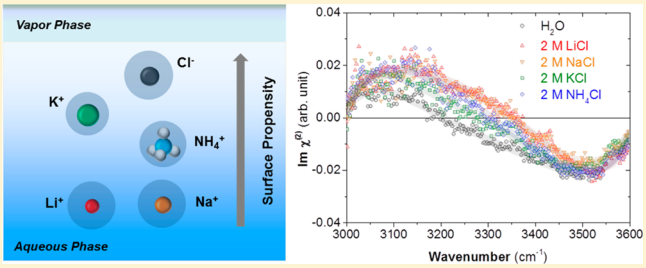

INTRODUCTION

Marine or sea salt aerosols (SSAs) originate mainly from turbulent wave action at the surface of oceans, more specifically through the bursting of bubbles formed by breaking waves.[1,2] Bubble rupture produces aerosol droplets with a size typically ranging from about 0.01 to 10 μm in diameter.[3−5] Depending on their size, these aerosols can have various atmospheric lifetimes and can travel great distances over continental regions by being entrained in an air mass.[6] Aerosols play a key role in the modification of global climate through their effect on cloud condensation nuclei, radiative balance, and level of precipitation.[7] Aerosol composition and size have also been correlated to thundercloud electrification and thunderstorm severity.[8,9]

The chemical components of newly formed SSAs reflect that of seawater enriched with inorganic salts, organic molecules (lipids, sterols, amino acids, etc.), cellular debris, and even living microorganisms that exist in the marine boundary layer (MBL).[10−12] However, heterogeneous reactions in the bulk and at the surface of SSAs modify their chemical composition in the atmosphere. In general, SSAs contain alkali metals (Na^+, K^+, Li^+), alkaline earth metals (Mg^{2+}, Ca^{2+}), as well as ammonium (NH_4^+) as the major cationic species, whereas halides (F^-, Cl^-, Br^-, and I^-) and oxidized sulfur and nitrogen ions make up the majority of anionic species.[13]

A detailed knowledge of halide anion distributions and of their countercations at the air/aqueous interface is thus of great importance for further understanding the chemistry of SSAs. The prevalent molecular picture of ion distributions at air/aqueous interfaces predicted by classical molecular dynamics (MD) simulations using polarizable force fields has the segregation of anions and cations in the interfacial region with larger and more polarizable anions (I^-, Br^-) significantly enriched in the topmost water layer, while smaller, less polarizable and/or highly charged anions (e.g., F^-) and cations (e.g., Li^+, Na^+, Mg^{2+}) are repelled from the surface and reside deeper below, thus forming in most cases an ionic double layer structure.[14−20] As for the Cl^- anion, recent MD simulations have suggested that it exhibits a somewhat "borderline" surface propensity, as it is neither depleted nor enhanced at the surface.[14,16,21,22]

A variety of experimental techniques have been deployed to study air/aqueous interfaces of halide salt solutions, including electrospray ionization-mass spectrometry (ESI-MS),[23,24] ambient pressure X-ray photoelectron spectroscopy (AP-XPS),[22,25−27] grazing incidence X-ray fluorescence,[28] X-ray reflectivity,[29] and surface-sensitive optical spectroscopies such as resonant and nonresonant second harmonic generation (SHG)[30−32] as well as vibrational sum frequency generation (VSFG)[33−38] and its phase-resolved variants, phase-sensitive (PS-) and heterodyne-detected (HD-)VSFG spectroscopy.[39−41] Aside from a few exceptions, most of these studies have lent support to the predicted physical picture of enhanced anion concentration in the interfacial region. For example,

Special Issue: James L. Skinner Festschrift

Received: March 29, 2014
Revised: May 5, 2014
Published: May 5, 2014

   dx.doi.org/10.1021/jp503132m | J. Phys. Chem. B 2014, 118, 8433−8440

using conventional VSFG spectroscopy on sodium halide solutions, Liu et al. observed a greater perturbation of interfacial water organization for NaBr and NaI than for NaCl or NaF relative to the neat air/water interface, suggesting that the extent of halide anion surface enhancement in the aqueous salt solutions increases with increasing anion size and polarizability ($I^- > Br^- > Cl^- > F^-$).[35] Wang and co-workers observed enhanced SHG signal concomitant with increasing bulk salt concentrations, indicative of an overall increase in the interfacial depth following the order NaBr > NaCl ≈ NaF.[31] Furthermore, Ghosal et al. have confirmed a similar anion surface enhancement at the air/aqueous interface of potassium halide salt solutions and showed that larger, more polarizable anions exhibited greater surface enhancement.[25] More recently, Shen and co-workers confirmed the influence of I^- anions on the hydrogen bonding structure of interfacial water of NaI salt solutions. They further suggested with PS-VSFG spectroscopy that the distribution of Na^+ and I^- ions may create an interfacial electric field that reorients part of the interfacial water molecules toward the vapor phase.[41] Taken together, all of these results have provided invaluable information concerning specific anion effects on the interfacial water molecules of halide salt solutions.[42]

In comparison to anions, the influence of cations on the interfacial water organization has been studied less. Typically, cations are thought to be repelled from the water surface. Nevertheless, due to the condition of electroneutrality that must be met, anions and cations would have the same concentration in the interfacial region, such that cations should be in the vicinity of the enhanced population of anions. Because of that, it has been suggested that cations could influence the surface propensity and stability of halide anions at the air/aqueous interface, which may, in turn, affect the interfacial water organization.[42]

As of now, few experimental studies have focused on the cation effects on the hydrogen bonding structure of interfacial water molecules.[32,37,39] For instance, it was shown for the series of NaX and KX (X = F^-, Cl^-, Br^-) salt solutions that, in addition to halide anion effects, unexpected specific Na^+ and K^+ cation effects also contributed in increasing the interfacial depth and in changing the orientational order of interfacial water molecules of aqueous solutions.[32] With the exception of fluoride salts, these effects were more pronounced for K^+ than for Na^+ and found to be due to the sum of the individual anion and cation contributions. In the case of NaF and KF solutions, stronger ion pairing effects have been invoked to explain the reversed behavior. Nevertheless, a cation-specific effect was also observed in the conventional VSFG spectra of these solutions which could not be explained on the current predicted molecular picture.[37] It was argued that even though F^- anion and Na^+, K^+ cation interfacial concentrations are diminished compared to the bulk concentration, these ions could still have some influence over the interfacial water molecules. These effects are not discussed to any extent in MD simulation studies, which treats F^- and both Na^+ and K^+ cations as small, rather nonpolarizable ions, and thus repelled from the air/aqueous interface.

Tian et al. also observed some cation specificity, albeit to a lesser extent, in the PS-VSFG spectra of NaCl, KCl, and NH_4Cl salt solutions.[39] A slightly more positive spectrum for NaCl and KCl solutions relative to that of neat water revealed the overall preferential orientation of interfacial water molecules due to the presence of weak negative electric fields induced by the formation of a double layer structure with Cl^- anions located above K^+ and Na^+ cations, respectively, in agreement with MD simulation predictions.[14,21,22,43,44] In contrast, NH_4Cl showed a more negative spectrum relative to neat water and hence a positive electric field caused by having NH_4^+ cations with a higher surface propensity than Cl^- anions, a result at odds with the predicted picture.[36] On the basis of the magnitude of the interfacial electric field, the combined ion (cation + anion) effect on the interfacial electric field can be ranked as $NH_4^+ > Na^+ \gtrsim K^+$. More recently, Hemminger and co-workers using AP-XPS and MD simulations demonstrated the existence of a cation-specific effect in concentrated NaCl and RbCl salt solutions where an increasing countercation size caused a decrease in Cl^- anion surface enhancement.[22] Interestingly, all the molecular-level information gathered so far seems to indicate that ion distributions and ion-specific effects at the air/aqueous interface of halide salt solutions are far more complex than expected.

In this work, the influence of monovalent alkali metal (Li^+, Na^+, K^+) and ammonium (NH_4^+) cations on the organization of interfacial water molecules is investigated with the help of conventional VSFG and HD-VSFG spectroscopy. According to our VSFG results, the perturbation of the interfacial water hydrogen bonding by monovalent cations in the OH stretching region was found to be more pronounced for LiCl and NH_4Cl solutions. The Im $\chi_s^{(2)}(\omega_{IR})$ spectra suggest the presence of a positive electric field for all chloride solutions whose direction is governed by an ionic double layer structure with Cl^- ions located above the countercations. However, the change in magnitude of the electric field shows that the orientation of the water OH transition dipole moments is mostly affected by monovalent cations in the following order: $Li^+ \approx Na^+ > NH_4^+ > K^+$. Furthermore, it was found for NH_4Cl salt solution that the surface propensity of Cl^- over NH_4^+ inferred in this work is in good agreement with MD simulation predictions but opposite to that presented by Tian et al.[39]

EXPERIMENTAL SECTION

Materials. LiCl (Fisher Scientific, 99% colorless crystals, Fisher BioReagents), NaCl (Fisher Scientific, ACS grade, >98%), KCl (Fisher Scientific, 99%), and NH_4Cl (MP Biomedicals, ultrapure grade, >99%) salts were pretreated according to procedures published previously to remove potential remaining organic contamination.[45] Ultrapure water with a resistivity of 18.2−18.3 MΩ·cm and a measured pH of ∼5.6 (the pH value is slightly acidic due to the dissolution of gaseous CO_2) was obtained from a Barnstead Nanopure system (model D4741, Thermolyne Corporation) equipped with additional organic removing cartridges (D5026 Type I ORGANICfree Cartridge Kit; Pretreat Feed).

Preparation of Salt Solutions. Stock salt solutions were prepared by dissolving pretreated salts in ultrapure water and then filtering them twice using activated carbon filters (Whatman Carbon Cap 75, Fisher Scientific) to completely eliminate organic impurities.[45] Concentrations of the chloride salt solutions were standardized by Mohr titration.[46] The measured pH of solutions laid in the range 5−7. All salt solutions were shown to be free of organic impurities, as revealed by their conventional VSFG spectra obtained in the surfactant CH stretching region (2800−3000 cm^{-1}) (Figure S1, Supporting Information). All solutions were thermally equilibrated to room temperature (23 ± 1 °C) over 24 h before use.

dx.doi.org/10.1021/jp503132m | J. Phys. Chem. B 2014, 118, 8433−8440

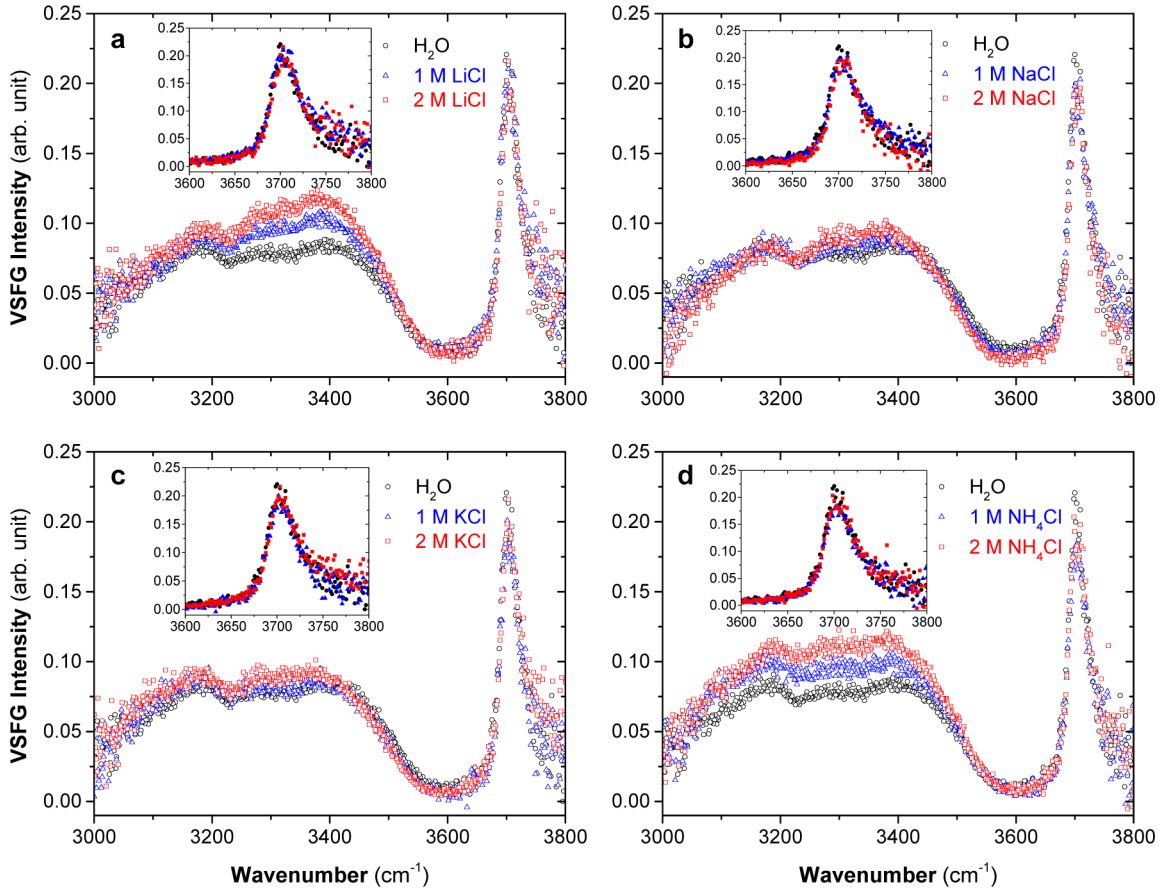

Figure 1. VSFG spectra of air/aqueous interfaces of 1 and 2 M chloride salt solutions in the water OH stretching region (3000−3800 cm^{-1}): (a) LiCl, (b) NaCl, (c) KCl, and (d) NH_4Cl. The VSFG spectrum of the neat air/water interface is also given as a reference. A close-up of the dangling OH peak for each solution is also shown in an inset.

Methods. Conventional and Heterodyne-Detected VSFG Spectroscopy. Conventional VSFG and HD-VSFG spectroscopy measurements were performed on a broad-bandwidth VSFG spectrometer setup that has been described in detail elsewhere.[47−49] The HD-VSFG measurements differ from the conventional VSFG only in the optical configuration of the sample stage area whose design is similar to the one reported by Tahara and co-workers.[50,51] The HD-VSFG setup and the data processing procedure used have been described previously.[40,43,52,53] Incident angles of visible and infrared beams were 59/63 ± 1 and 50/60 ± 1° for the conventional VSFG and HD-VSFG experiments, respectively. The ssp (s for sum-frequency, s for visible, and p for infrared) polarization configuration was chosen, and the average incident energy of the visible (0.8 μm) and infrared (2.6−3.3 μm in the water OH stretching region) beams impinging on the aqueous surface was 300 and 10 μJ for the VSFG measurements and 260 and 8 μJ for HD-VSFG. The measured VSFG spectra of the different air/aqueous interfaces were normalized against a reference GaAs(110) crystal. In the case of HD-VSFG spectra, the normalization was done against a reference quartz crystal. Neat water spectra were used as a reference for salt comparison to assess reproducibility during the entire experimental period. The reproducibility for both conventional VSFG and Im $\chi_s^{(2)}(\omega_{IR})$ spectra of neat water is demonstrated in the Supporting Information. All Im $\chi_s^{(2)}(\omega_{IR})$ spectra of salt solutions are compared to the one of neat water such that their interpretation is mainly based on the relative difference between neat water and the salt solutions. The consistency and trends of these spectra were checked by comparing the deduced power $|\chi_s^{(2)}(\omega_{IR})|^2$ spectrum of each salt solution to that measured directly by conventional VSFG spectroscopy (data not shown). Only every second and fourth data points are plotted in the conventional VSFG and HD-VSFG spectra, respectively, to avoid spectral clutter.

RESULTS AND DISCUSSION

Cation Effects on the Interfacial Water Hydrogen-Bonding Network. VSFG spectra of the interfacial region of 1 and 2 M LiCl, NaCl, KCl, and NH_4Cl aqueous salt solutions are shown in Figure 1. The interfacial region refers hereafter to the region that lacks inversion symmetry, hence is SFG-active. In the case of neat water, only the topmost layers (∼1−3) are believed to be responsible for the observed SFG signal, while the adjacent sublayers make little contribution;[41,54] however, the presence of ions generates an interfacial electric field by forming an ionic double layer which extends the region of noncentrosymmetry.[55] The VSFG spectrum of the neat air/water interface is also given as a reference for all salt solution spectra. The neat water spectrum reveals a broad region spanning from 3000 to 3600 cm^{-1} representing coordinated water molecules with a broad continuum of hydrogen bond lengths and strengths and a narrow band at 3700 cm^{-1} assigned to the distinct dangling OH bond of water molecules located in the topmost layer. In the lower frequency part of the broad region, it is accepted that hydrogen bonds are relatively strong,

dx.doi.org/10.1021/jp503132m | J. Phys. Chem. B 2014, 118, 8433−8440

and as one moves to higher frequency, the hydrogen bonding strength weakens significantly. Other interpretations and assignments for this broad continuum have also been proposed.[56−64] The presence and distribution of ions in the interfacial region can affect the VSFG water spectrum either by changing (i) the number of contributing water molecules, (ii) their orientation, and/or (iii) their OH transition dipole strength from ion−water interactions.

As seen in Figure 1, the dissolution of chloride salts affects the interfacial water hydrogen-bonding network, albeit to different extents, depending on the cation identity and salt concentration. For example, the VSFG spectra of LiCl and NH_4Cl solutions display an uneven increase in intensity in the broad OH-bonded region from 3100 to 3500 cm^{-1} (Figure 1a,d), while comparatively only weaker changes are observed for NaCl and KCl solutions (Figure 1b,c). With the exception of LiCl for which no VSFG data has so far been reported, the results obtained for the other solutions are somewhat consistent with those previously published in the same concentration range.[16,33−36,39,40] It was suggested that the absence of appreciable changes observed for NaCl and KCl solutions indicates the presence of a weak interfacial field due to Na^+, K^+, and Cl^- repelled from the surface. Significant spectral changes in the OH-bonded region have been observed only for highly concentrated NaCl solutions.[55] MD simulations of low concentration (≤2 M) chloride salt solutions have predicted that Na^+ and K^+ cations are depleted in the interfacial region, while Cl^- anions are neither depleted nor enhanced.[15,16,21,22] By comparing the effect of the chloride salt solutions on the broad OH-bonded region (Figure 2), one can observe only a weak cation specificity in the perturbation of interfacial water molecules by monovalent cations following the order NH_4Cl > LiCl > NaCl ≈ KCl.

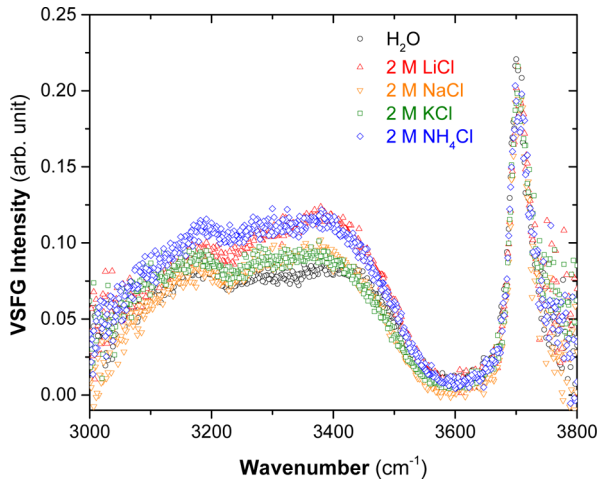

Figure 2. Comparison between conventional VSFG spectra of air/aqueous interfaces of 2 M chloride salt solutions in the water OH stretching region (3000−3800 cm^{-1}). The conventional VSFG spectrum of the neat air/water interface is also given as a reference.

In contrast, the intensity of the dangling OH peak appears to not be significantly affected relative to neat water in the presence of chloride salts in this concentration range (insets of Figure 1). This is consistent with previously published data that show no marked decrease in intensity at these concentrations. It is expected that a decrease in intensity of this peak should become significant at much higher salt concentrations where ion pairing effects become important, as was shown by Allen and co-workers with concentrated (∼5 M) NaCl solution.[55] This effect is even more pronounced in the case of divalent alkaline earth cations such as Mg^{2+} [38,65] and Ca^{2+} and will be addressed in a forthcoming publication.

Bulk IR and Raman spectra were also obtained for the salt solutions studied here (Figures S4−S7, Supporting Information). The trend relative to neat water observed in the conventional VSFG spectra of the surface of aqueous chloride salt solutions does not completely correlate with those from the corresponding bulk IR and Raman spectra. By comparison with the VSFG results, a similar trend (increased intensity) relative to water was only observed in the IR and Raman spectra around 3400 cm^{-1} for the LiCl, NaCl, and KCl solutions; however, in these spectra, the intensity increase of the NH_4Cl solution spectrum was the weakest, consistent with less charge transfer effects[66] and the ability for NH_4^+ to hydrogen bond with surrounding water molecules. An enhancement in the low frequency tail is also observed due to contributions of the NH_4^+ asymmetric and symmetric stretching modes as well as the bending−rocking mode combination.[36] A similar enhancement was also observed in the NH_4Cl IR spectrum.[36,67] As for the aqueous alkali chloride salt solutions, the OH stretching region (3100−3800 cm^{-1}) was mostly affected by the salt addition. Previous IR and Raman studies on aqueous alkali chloride solutions at different salt concentrations have shown spectral differences in the intensity of (1) the two water bands at ∼3200 and ∼3400 cm^{-1} and, concomitantly, (2) the weak shoulder near 3650 cm^{-1}.[68−72] The former bands have been assigned to water molecules fully hydrogen-bonded to their nearest neighbors, whereas the latter has been associated with water molecules very weakly hydrogen-bonded (sometimes referred to as quasi-"free OH"). Reported results have shown that bulk Raman spectra of alkali chloride salt solutions are quite different from that of pure water; however, no significant cation effect was detected in the OH stretching and bending (∼1645 cm^{-1}) regions.[68,72] The insensitivity of water intramolecular Raman vibrations to cations has been ascribed to the predominantly electrostatic interactions between alkali cations and lone-pair electrons of water's oxygen.[68]

Cation Effects on the Interfacial Electric Field. The Im $\chi_s^{(2)}(\omega_{IR})$ spectra of the air/aqueous interfaces of LiCl, NaCl, KCl, and NH_4Cl salt solutions are shown in Figure 3. In comparison to the conventional VSFG spectroscopy, HD-VSFG directly provides the sign and thus the net orientation of the water OH transition dipole moment of SFG-active OH vibrational stretching modes. The Im $\chi_s^{(2)}(\omega_{IR})$ spectrum of the neat air/water in the OH stretching region is shown in Figure 3. The sign of the $\chi_s^{(2)}(\omega_{IR})$ spectrum of neat water in the 3000−3200 cm^{-1} region is positive, suggesting that the OH stretch net transition dipole moment is oriented toward the surface; however, the assignment of absolute orientation for this region has not been fully explained by recent theoretical predictions.[59,62,73] In contrast, the Im $\chi_s^{(2)}(\omega_{IR})$ spectrum from 3200 to 3600 cm^{-1} reveals a negative band, and this spectral region interpretation is not contested. Although the orientational distribution is likely to be broad, the OH stretches in this frequency range have a net transition dipole moment oriented on average toward the isotropic bulk solution.

Relative to neat water, a positive increase in signal intensity can be observed from 3200 to ∼3500 cm^{-1} for all chloride solutions but to different extents depending on the cation identity (Figure 3). Aside from a larger signal intensity relative

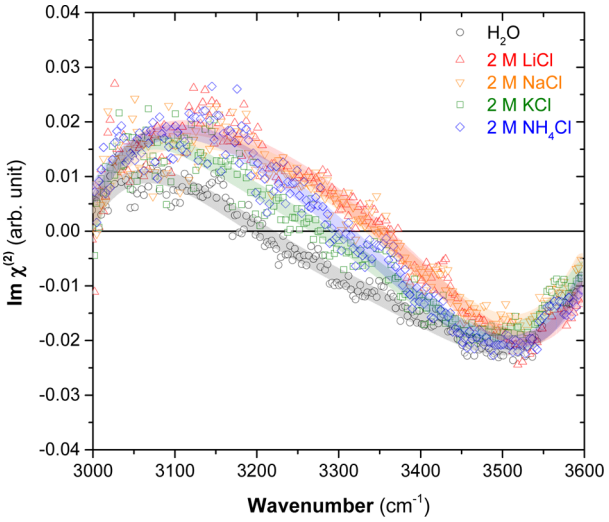

Figure 3. Comparison between Im $\chi_s^{(2)}(\omega_{IR})$ spectra of air/aqueous interfaces of 2 M chloride salt solutions in the water OH stretching region (3000−3800 cm^{-1}). The Im $\chi_s^{(2)}(\omega_{IR})$ spectrum of the neat air/water interface is also given as a reference. The solid curves serve as eye guides to show the trend in the data.

to water, the overall profile and trend of the NaCl and KCl solution Im $\chi_s^{(2)}(\omega_{IR})$ spectra presented here are in good agreement with those previously reported by Tian et al. at the same concentrations;[39] again, up until now, there has been no published account of an Im $\chi_s^{(2)}(\omega_{IR})$ spectrum from the air/aqueous interface of LiCl solutions. The overall positive enhancement can be interpreted physically by the generation of a positive (here the E-field direction is defined going from positive to negative charge distributions) electric field induced by an ionic double layer formed between Cl^- anions located predominantly above their countercations, closer to the surface. The presence of this ion-induced electric field, in turn, leads to a reorganization of the hydrogen-bonding network and to the reorientation of more interfacial water molecules with their net OH transition dipole moment now preferentially directed toward the surface. This molecular picture is consistent with MD simulations of the air/aqueous interface of alkali chloride salt solutions which predicts the formation of a double layer structure with Cl^- ion having a greater surface propensity.[14,21,22,43,44] The trend seen in Figure 3 in the 3100−3500 cm^{-1} region definitely reveals the presence of a small cation effect on the magnitude of the interfacial electric field that follows the order $Li^+ \approx Na^+ > NH_4^+ > K^+$. This result agrees remarkably well with the corresponding small cation effect (but following the reversed trend because of the relation $\Delta V = -\int E(z)\,dz$) that was previously observed in surface potential difference measurements of aqueous alkali chloride solutions in the same concentration range.[74−76] Interestingly, the trend revealed in Figure 3 somewhat differs from the one observed in Figure 2, especially for NH_4^+. This apparent discrepancy could be the result from complications of the convolution between the Im $\chi_s^{(2)}(\omega_{IR})$ and Re $\chi_s^{(2)}(\omega_{IR})$ contributions as well as between nonresonant and resonant contributions in the measured VSFG spectra (Figure S3, Supporting Information).[53]

The difference in the Im $\chi_s^{(2)}(\omega_{IR})$ signal intensity for each salt solution can be attributed to the orientational polarization effect on the interfacial water OH transition dipole moments caused by the electrostatic field generated by the ionic double layer. Generally, the magnitude of this field will depend on the different ion density profiles, i.e., the accumulation/depletion of one ionic species relative to the other as well as the spatial separation between the maxima of anion and cation distributions. For example, the Im $\chi_s^{(2)}(\omega_{IR})$ spectra of 2 M NaCl and KCl solutions suggest that Cl^- anions have a greater surface propensity than Na^+ and K^+, thus leading to the formation of an ionic double layer structure with a positive electric field that orients more effectively water OH transition dipole moments toward the vapor phase. However, the magnitude of the E-field must still be relatively weak, since it remains insufficient to reorient the OH dipole moment of water species associated with the spectral region beyond ~3350 cm^{-1}. This would be qualitatively consistent with previous MD simulations of NaCl and KCl solutions that predicted similar and somewhat closely spaced anion and cation density profiles, both enriched below the Gibbs dividing surface; as expected, Na^+ and K^+ are repelled further from the interface than Cl^-.[14,21,43,44] The difference in signal enhancement between NaCl and KCl could originate from different E-field magnitudes but also from a difference in interfacial depth. However, because the concentration (accumulation or depletion) of Cl^- anions, the separation of the peak profiles, as well as the extent of interfacial depth depend to some extent on the polarizable force field models considered, it remains at present difficult to unravel the origin(s) of the cation effect simply based on the comparison of currently available NaCl and KCl profiles. The case of LiCl solutions is particularly interesting. Even though Li^+ exhibits a greater surface charge density than Na^+ and should be repelled deeper in the interfacial region due to unfavorable image charge interactions, however, their Im $\chi_s^{(2)}(\omega_{IR})$ spectra are practically identical. Surface potential data for these solutions at similar concentrations are also indistinguishable.[74] Following the previous argument, this would mean that the Li^+/Cl^- and Na^+/Cl^- profiles are similar. Although to our knowledge no MD simulation of the air/aqueous interface of LiCl solutions has been performed, according to an argument proposed by Netz and co-workers, the peculiar surface propensity of Li^+ could be due to the strong binding of the first solvation shell, making Li^+ appear larger and less repelled from the interface.[77] In this case, the lower electrostatic penalty outweighs the free energy cost associated with the creation of a larger ionic cavity volume. This is also supported by double difference IR spectroscopy studies on alkali perchlorate salts that indicated the presence of two hydration shells in the case of Li^+ cations compared to Na^+, which could more effectively screen the Li^+ ion surface charge.[78]

Like the other alkali metal chloride solutions, the Im $\chi_s^{(2)}(\omega_{IR})$ spectrum of the 2 M NH_4Cl also shows a positive deviation relative to water; this result, however, agrees only partially with that of Tian et al. which showed a negative deviation in the spectral region from ~3275 to 3500 cm^{-1}.[39] At present, it appears difficult to settle this discrepancy. A possible explanation could come from the different salt grades and purification procedures used in the treatment of salts and salt solutions which have been shown to be critical in the spectroscopic investigations of aqueous interfaces.[45] Due to the NH_4Cl salt low melting point, purification of its aqueous solution can only be done through extensive filtration. In contrast, better agreement between the two sets of experiments can be found for alkali chloride salts which can undergo baking and/or solution filtration. Nevertheless, the average orientation of the water OH transition dipole moments in the NH_4Cl

dx.doi.org/10.1021/jp503132m | J. Phys. Chem. B 2014, 118, 8433−8440

solution indicates that, similarly to NaCl, Cl^- anions also have a greater surface propensity than NH_4^+. However, the lower magnitude of the E-field inferred from the present work would suggest a smaller separation between both peak density profiles. This picture is supported by available MD simulations which show that NH_4^+ cations move closer by about 1 Å to the surface than Na^+.[36] A similar distribution is also predicted for sulfate salts, even though SO_4^{2-} divalent anions are solvated deeper than Cl^- in the interfacial region.[36] Further systematic theoretical exploration of the interfacial ion distribution of alkali and alkaline earth salt series is certainly warranted, as it would give further insight into the molecular factors behind the cation-specific effects.

CONCLUSIONS

The influence of monovalent cations on interfacial water organization of aqueous chloride (LiCl, NaCl, KCl, and NH_4Cl) solutions was examined using conventional VSFG and HD-VSFG spectroscopy. To the author's knowledge, this is the first time that the spectra of LiCl solutions have been reported. The conventional VSFG spectra reveal only a weak cation-specific effect with LiCl and NH_4Cl being the only salts significantly affecting interfacial water organization. However, and more accurate, the Im $\chi_s^{(2)}(\omega_{IR})$ obtained from all chloride salt solutions showed a small cation-specific effect for all cations measured relative to the neat air/water interface. The positive enhancement of the Im $\chi_s^{(2)}(\omega_{IR})$ signal follows the order $Li^+ \approx Na^+ > NH_4^+ > K^+$. The trend in the magnitude of the inferred electric field is in good agreement with that of previously published surface potential data. In addition, the direction of the electric field suggests that Cl^- ions are always located above the countercations, even in the case of NH_4Cl salt solution, in contrast with previously reported HD-VSFG data. The molecular picture of the relative surface propensity of Cl^- and cations is in agreement with predictions of MD simulations. The influence of divalent cations on the interfacial water organization will be explored in a forthcoming publication.

ASSOCIATED CONTENT

Supporting Information

Conventional VSFG spectra of filtered stock salt solutions examined in the surfactant CH stretching region (2800−3000 cm^{-1}) showing the absence of organic contamination. GaAs profile and conventional VSFG and HD-VSFG Im $\chi_s^{(2)}(\omega_{IR})$ spectra of neat water in the water OH stretching region obtained through the entire experimental period demonstrating system and phase stability. Re $\chi_s^{(2)}(\omega_{IR})$ spectra deduced from HD-VSFG results of water molecules at the air/aqueous interface of chloride salt solutions. Experimental details of IR and Raman spectroscopy as well as bulk Raman and IR spectra of all chloride salt solutions in the water OH stretching region. This material is available free of charge via the Internet at http://pubs.acs.org.

AUTHOR INFORMATION

Corresponding Author

*E-mail: allen@chemistry.ohio-state.edu.

Notes

The authors declare no competing financial interest.

ACKNOWLEDGMENTS

The authors acknowledge NSF-CHE (Grant No. CHE-1111762) for funding this work. W.H. acknowledges a Presidential Fellowship from The Ohio State University.

REFERENCES

(1) Prospero, J. M. *The Chemical and Physical Properties of Marine Aerosols: An Introduction, in Chemistry of Marine Water and Sediments*; Springer-Verlag: Berlin, Heidelberg, 2002; pp 35−82.
(2) Lewis, E. R.; Schwartz, S. E. *Sea Salt Aerosols Production: Mechanisms, Methods, Measurements and Models*; American Geophysical Union: Washington, DC, 2004.
(3) Fitzgerald, J. W. Marine Aerosols - A Review. *Atmos. Environ.* **1991**, *25*, 533−545.
(4) O'Dowd, C. D.; Smith, M. H.; Consterdine, I. E.; Lowe, J. A. Marine Aerosol, Sea-Salt, and the Marine Sulphur Cycle: A Short Review. *Atmos. Environ.* **1997**, *31*, 73−80.
(5) Bates, T. S.; Kapustin, V. N.; Quinn, P. K.; Covert, D. S.; Coffman, D. J.; Mari, C.; Durkee, P. A.; De Bruyn, W. J.; Saltzman, E. S. Processes Controlling the Distribution of Aerosol Particles in the Lower Marine Boundary Layer During the First Aerosol Characterization Experiment (ACE-1). *J. Geophys. Res.: Atmos.* **1998**, *103*, 16369−16383.
(6) Shaw, G. E. Aerosol Chemical Components in Alaska Air Masses: 2. Sea Salt and Marine Products. *J. Geophys. Res.: Atmos.* **1991**, *96*, 22369−22372.
(7) Forster, P.; Ramaswamy, V.; Artaxo, P.; Berntsen, T.; Betts, R.; Fahey, D. W.; Haywood, J.; Lean, J.; Lowe, D. C.; Myhre, G. et al. Changes in Atmospheric Constituents and in Radiative Forcing. *Climate Change 2007: The Physical Science Basis. Contribution of Working Group I to the Fourth Assessment Report of the Intergovernmental Panel on Climate Change*; Cambridge University Press: Cambridge, U.K., New York, 2007; pp 129−234.
(8) Rosenfeld, D.; Lohmann, U.; Raga, G. B.; O'Dowd, C. D.; Kulmala, M.; Fuzzi, S.; Reissell, A.; Andreae, M. O. Flood or Drought: How Do Aerosols Affect Precipitation? *Science* **2008**, *321*, 1309−1313.
(9) Jungwirth, P.; Rosenfeld, D.; Buch, V. A Possible New Molecular Mechanism of Thundercloud Electrification. *Atmos. Res.* **2005**, *76*, 190−205.
(10) O'Dowd, C. D.; Facchini, M. C.; Cavalli, F.; Ceburnis, D.; Mircea, M.; Decesari, S.; Fuzzi, S.; Yoon, Y. J.; Putaud, J. P. Biogenically Driven Organic Contribution to Marine Aerosol. *Nature* **2004**, *431*, 676−680.
(11) Li, Y.; Ezell, M. J.; Finlayson-Pitts, B. J. The Impact of Organic Coatings on Light Scattering by Sodium Chloride Particles. *Atmos. Environ.* **2011**, *45*, 4123−4132.
(12) Ault, A. P.; Moffet, R. C.; Baltrusaitis, J.; Collins, D. B.; Ruppel, M. J.; Cuadra-Rodriguez, L. A.; Zhao, D. F.; Guasco, T. L.; Ebben, C. J.; Geiger, F. M.; et al. Size-Dependent Changes in Sea Spray Aerosol Composition and Properties with Different Seawater Conditions. *Environ. Sci. Technol.* **2013**, *47*, 5603−5612.
(13) Millero, F. J. *Chemical Oceanography*, 4th ed.; CRC Press: Boca Raton, FL, 2013.
(14) Jungwirth, P.; Tobias, D. J. Molecular Structure of Salt Solutions: A New View of the Interface with Implications for Heterogeneous Atmospheric Chemistry. *J. Phys. Chem. B* **2001**, *105*, 10468−10472.
(15) Jungwirth, P.; Tobias, D. J. Ions at the Air/Water Interface. *J. Phys. Chem. B* **2002**, *106*, 6361−6373.
(16) Mucha, M.; Frigato, T.; Levering, L. M.; Allen, H. C.; Tobias, D. J.; Dang, L. X.; Jungwirth, P. Unified Molecular Picture of the Surfaces of Aqueous Acid, Base, and Salt Solutions. *J. Phys. Chem. B* **2005**, *109*, 7617−7623.
(17) Chang, T. M.; Dang, L. X. Recent Advances in Molecular Simulations of Ion Solvation at Liquid Interfaces. *Chem. Rev.* **2006**, *106*, 1305−1322.

(18) Jungwirth, P.; Winter, B. Ions at Aqueous Interfaces: From Water Surface to Hydrated Proteins. *Annu. Rev. Phys. Chem.* **2008**, *59*, 343−366.
(19) Jungwirth, P. Spiers Memorial Lecture Ions at Aqueous Interfaces. *Faraday Discuss.* **2009**, *141*, 9−30.
(20) Tobias, D. J.; Stern, A. C.; Baer, M. D.; Levin, Y.; Mundy, C. J. Simulation and Theory of Ions at Atmospherically Relevant Aqueous Liquid-Air Interfaces. *Annu. Rev. Phys. Chem.* **2013**, *64*, 339−359.
(21) Wick, C. D.; Dang, L. X.; Jungwirth, P. Simulated Surface Potentials at the Vapor-Water Interface for the KCl Aqueous Electrolyte Solution. *J. Chem. Phys.* **2006**, *125*, 024706/1−024706/4.
(22) Cheng, M. H.; Callahan, K. M.; Margarella, A. M.; Tobias, D. J.; Hemminger, J. C.; Bluhm, H.; Krisch, M. J. Ambient Pressure X-Ray Photoelectron Spectroscopy and Molecular Dynamics Simulation Studies of Liquid/Vapor Interfaces of Aqueous NaCl, RbCl, and RbBr Solutions. *J. Phys. Chem. C* **2012**, *116*, 4545−4555.
(23) Cheng, J.; Vecitis, C. D.; Hoffmann, M. R.; Colussi, A. J. Experimental Anion Affinities for the Air/Water Interface. *J. Phys. Chem. B* **2006**, *110*, 25598−25602.
(24) Enami, S.; Colussi, A. J. Long-Range Specific Ion-Ion Interactions in Hydrogen-Bonded Liquid Films. *J. Chem. Phys.* **2013**, *138*, 184706/1−184706/6.
(25) Ghosal, S.; Hemminger, J. C.; Bluhm, H.; Mun, B. S.; Hebenstreit, E. L. D.; Ketteler, G.; Ogletree, D. F.; Requejo, F. G.; Salmeron, M. Electron Spectroscopy of Aqueous Solution Interfaces Reveals Surface Enhancement of Halides. *Science* **2005**, *307*, 563−566.
(26) Winter, B.; Faubel, M. Photoemission from Liquid Aqueous Solutions. *Chem. Rev.* **2006**, *106*, 1176−1211.
(27) Brown, M. A.; D'Auria, R.; Kuo, I. F. W.; Krisch, M. J.; Starr, D. E.; Bluhm, H.; Tobias, D. J.; Hemminger, J. C. Ion Spatial Distributions at the Liquid-Vapor Interface of Aqueous Potassium Fluoride Solutions. *Phys. Chem. Chem. Phys.* **2008**, *10*, 4778−4784.
(28) Padmanabhan, V.; Daillant, J.; Belloni, L.; Mora, S.; Alba, M.; Konovalov, O. Specific Ion Adsorption and Short-Range Interactions at the Air Aqueous Solution Interface. *Phys. Rev. Lett.* **2007**, *99*, 086105/1−086105/4.
(29) Sloutskin, E.; Baumert, J.; Ocko, B. M.; Kuzmenko, I.; Checco, A.; Tamam, L.; Ofer, E.; Gog, T.; Gang, O.; Deutsch, M. The Surface Structure of Concentrated Aqueous Salt Solutions. *J. Chem. Phys.* **2007**, *126*, 054704/1−054704/10.
(30) Petersen, P. B.; Saykally, R. J. Probing the Interfacial Structure of Aqueous Electrolytes with Femtosecond Second Harmonic Generation Spectroscopy. *J. Phys. Chem. B* **2006**, *110*, 14060−14073.
(31) Bian, H.-t.; Feng, R.-r.; Xu, Y.-y.; Guo, Y.; Wang, H.-f. Increased Interfacial Thickness of the NaF, NaCl and NaBr Salt Aqueous Solutions Probed with Non-Resonant Surface Second Harmonic Generation (SHG). *Phys. Chem. Chem. Phys.* **2008**, *10*, 4920−4931.
(32) Bian, H. T.; Feng, R. R.; Guo, Y.; Wang, H. F. Specific Na^+ and K^+ Cation Effects on the Interfacial Water Molecules at the Air/Aqueous Salt Solution Interfaces Probed with Nonresonant Second Harmonic Generation. *J. Chem. Phys.* **2009**, *130*, 134709/1−134709/11.
(33) Schnitzer, C. S.; Baldelli, S.; Shultz, M. J. Sum Frequency Generation of Water on NaCl, $NaNO_3$, $KHSO_4$, HCl, HNO_3, and H_2SO_4 Aqueous Solutions. *J. Phys. Chem. B* **2000**, *104*, 585−590.
(34) Raymond, E. A.; Richmond, G. L. Probing the Molecular Structure and Bonding of the Surface of Aqueous Salt Solutions. *J. Phys. Chem. B* **2004**, *108*, 5051−5059.
(35) Liu, D.; Ma, G.; Levering, L. M.; Allen, H. C. Vibrational Spectroscopy of Aqueous Sodium Halide Solutions and Air-Liquid Interfaces: Observation of Increased Interfacial Depth. *J. Phys. Chem. B* **2004**, *108*, 2252−2260.
(36) Gopalakrishnan, S.; Jungwirth, P.; Tobias, D. J.; Allen, H. C. Air-Liquid Interfaces of Aqueous Solution Containing Ammonium and Sulfate: Spectroscopic and Molecular Dynamics Studies. *J. Phys. Chem. B* **2005**, *109*, 8861−8872.
(37) Feng, R.-r.; Bian, H.-t.; Guo, Y.; Wang, H.-f. Spectroscopic Evidence for the Specific Na^+ and K^+ Interactions with the Hydrogen-Bonded Water Molecules at the Electrolyte Aqueous Solution Surfaces. *J. Chem. Phys.* **2009**, *130*, 134710/1−134710/6.
(38) Casillas-Ituarte, N. N.; Callahan, K. M.; Tang, C. Y.; Chen, X. K.; Roeselova, M.; Tobias, D. J.; Allen, H. C. Surface Organization of Aqueous $MgCl_2$ and Application to Atmospheric Marine Aerosol Chemistry. *Proc. Natl. Acad. Sci. U.S.A.* **2010**, *107*, 6616−6621.
(39) Tian, C. S.; Byrnes, S. J.; Han, H. L.; Shen, Y. R. Surface Propensities of Atmospherically Relevant Ions in Salt Solutions Revealed by Phase-Sensitive Sum Frequency Vibrational Spectroscopy. *J. Phys. Chem. Lett.* **2011**, *2*, 1946−1949.
(40) Hua, W.; Jubb, A. M.; Allen, H. C. Electric Field Reversal of Na_2SO_4, $(NH_4)_2SO_4$, and Na_2CO_3 Relative to $CaCl_2$ and NaCl at the Air/Aqueous Interface Revealed by Heterodyne-Detected Phase-Sensitive Sum Frequency. *J. Phys. Chem. Lett.* **2011**, *2*, 2515−2520.
(41) Ji, N.; Ostroverkhov, V.; Tian, C. S.; Shen, Y. R. Characterization of Vibrational Resonances of Water-Vapor Interfaces by Phase-Sensitive Sum-Frequency Spectroscopy. *Phys. Rev. Lett.* **2008**, *100*, 096102/1−096102/4.
(42) Jungwirth, P.; Tobias, D. J. Specific Ion Effects at the Air/Water Interface. *Chem. Rev.* **2006**, *106*, 1259−1281.
(43) Ishiyama, T.; Morita, A. Molecular Dynamics Study of Gas-Liquid Aqueous Sodium Halide Interfaces. I. Flexible and Polarizable Molecular Modeling and Interfacial Properties. *J. Phys. Chem. C* **2007**, *111*, 721−737.
(44) Warren, G. L.; Patel, S. Comparison of the Solvation Structure of Polarizable and Nonpolarizable Ions in Bulk Water and Near the Aqueous Liquid-Vapor Interface. *J. Phys. Chem. C* **2008**, *112*, 7455−7467.
(45) Hua, W.; Verreault, D.; Adams, E. M.; Huang, Z. S.; Allen, H. C. Impact of Salt Purity on Interfacial Water Organization Revealed by Conventional and Phase-Sensitive Sum Frequency Generation Spectroscopy. *J. Phys. Chem. C* **2013**, *117*, 19577−19585.
(46) Finlayson, A. C. The pH Range of the Mohr Titration for Chloride-Ion Can Be Usefully Extended to 4−10.5. *J. Chem. Educ.* **1992**, *69*, 559.
(47) Hommel, E. L.; Allen, H. C. Broadband Sum Frequency Generation with Two Regenerative Amplifiers: Temporal Overlap of Femtosecond and Picosecond Light Pulses. *Anal. Sci.* **2001**, *17*, 137−139.
(48) Ma, G.; Allen, H. C. Surface Studies of Aqueous Methanol Solutions by Vibrational Broad Bandwidth Sum Frequency Generation Spectroscopy. *J. Phys. Chem. B* **2003**, *107*, 6343−6349.
(49) Tang, C. Y.; Allen, H. C. Ionic Binding of Na^+ Versus K^+ to the Carboxylic Acid Headgroup of Palmitic Acid Monolayers Studied by Vibrational Sum Frequency Generation Spectroscopy. *J. Phys. Chem. A* **2009**, *113*, 7383−7393.
(50) Nihonyanagi, S.; Yamaguchi, S.; Tahara, T. Direct Evidence for Orientational Flip-Flop of Water Molecules at Charged Interfaces: A Heterodyne-Detected Vibrational Sum Frequency Generation Study. *J. Chem. Phys.* **2009**, *130*, 204704/1−204704/5.
(51) Nihonyanagi, S.; Yamaguchi, S.; Tahara, T. Water Hydrogen Bond Structure near Highly Charged Interfaces Is Not Like Ice. *J. Am. Chem. Soc.* **2010**, *132*, 6867−6869.
(52) Chen, X. K.; Hua, W.; Huang, Z. S.; Allen, H. C. Interfacial Water Structure Associated with Phospholipid Membranes Studied by Phase-Sensitive Vibrational Sum Frequency Generation Spectroscopy. *J. Am. Chem. Soc., 132*, 11336−11342.
(53) Hua, W.; Chen, X. K.; Allen, H. C. Phase-Sensitive Sum Frequency Revealing Accommodation of Bicarbonate Ions, and Charge Separation of Sodium and Carbonate Ions within the Air/Water Interface. *J. Phys. Chem. A* **2011**, *115*, 6233−6238.
(54) Morita, A.; Hynes, J. T. A Theoretical Analysis of the Sum Frequency Generation Spectrum of the Water Surface. *Chem. Phys.* **2000**, *258*, 371−390.
(55) Allen, H. C.; Casillas-Ituarte, N. N.; Sierra-Hernandez, M. R.; Chen, X. K.; Tang, C. Y. Shedding Light on Water Structure at Air-Aqueous Interfaces: Ions, Lipids, and Hydration. *Phys. Chem. Chem. Phys.* **2009**, *11*, 5538−5549.

(56) Walker, D. S.; Hore, D. K.; Richmond, G. L. Understanding the Population, Coordination, and Orientation of Water Species Contributing to the Nonlinear Optical Spectroscopy of the Vapor-Water Interface through Molecular Dynamics Simulations. *J. Phys. Chem. B* **2006**, *110*, 20451−20459.
(57) Tian, C. S.; Shen, Y. R. Sum-Frequency Vibrational Spectroscopic Studies of Water/Vapor Interfaces. *Chem. Phys. Lett.* **2009**, *470*, 1−6.
(58) Sovago, M.; Campen, R. K.; Bakker, H. J.; Bonn, M. Hydrogen Bonding Strength of Interfacial Water Determined with Surface Sum-Frequency Generation. *Chem. Phys. Lett.* **2009**, *470*, 7−12.
(59) Ishiyama, T.; Morita, A. Analysis of Anisotropic Local Field in Sum Frequency Generation Spectroscopy with the Charge Response Kernel Water Model. *J. Chem. Phys.* **2009**, *131*, 244714/1−244714/7.
(60) Auer, B. M.; Skinner, J. L. Water: Hydrogen Bonding and Vibrational Spectroscopy, in the Bulk Liquid and at the Liquid/Vapor Interface. *Chem. Phys. Lett.* **2009**, *470*, 13−20.
(61) Fan, Y. B.; Chen, X.; Yang, L. J.; Cremer, P. S.; Gao, Y. Q. On the Structure of Water at the Aqueous/Air Interface. *J. Phys. Chem. B* **2009**, *113*, 11672−11679.
(62) Pieniazek, P. A.; Tainter, C. J.; Skinner, J. L. Surface of Liquid Water: Three-Body Interactions and Vibrational Sum-Frequency Spectroscopy. *J. Am. Chem. Soc.* **2011**, *133*, 10360−10363.
(63) Pieniazek, P. A.; Tainter, C. J.; Skinner, J. L. Interpretation of the Water Surface Vibrational Sum-Frequency Spectrum. *J. Chem. Phys.* **2011**, *135*, 044701/1−044701/12.
(64) Skinner, J. L.; Pieniazek, P. A.; Gruenbaum, S. M. Vibrational Spectroscopy of Water at Interfaces. *Acc. Chem. Res.* **2012**, *45*, 93−100.
(65) Callahan, K. M.; Casillas-Ituarte, N. N.; Xu, M.; Roeselova, M.; Allen, H. C.; Tobias, D. J. Effect of Magnesium Cation on the Interfacial Properties of Aqueous Salt Solutions. *J. Phys. Chem. A* **2010**, *114*, 8359−8368.
(66) Geissler, P. L. Water Interfaces, Solvation, and Spectroscopy. *Annu. Rev. Phys. Chem.* **2013**, *64*, 317−337.
(67) Max, J. J.; Chapados, C. Aqueous Ammonia and Ammonium Chloride Hydrates: Principal Infrared Spectra. *J. Mol. Struct.* **2013**, *1046*, 124−135.
(68) Yoshimura, Y.; Kanno, H. Cationic Effects in the Raman OD Stretching Spectra of Aqueous Electrolyte Solutions. *J. Raman Spectrosc.* **1996**, *27*, 671−674.
(69) Max, J. J.; Chapados, C. IR Spectroscopy of Aqueous Alkali Halide Solutions: Pure Salt-Solvated Water Spectra and Hydration Numbers. *J. Chem. Phys.* **2001**, *115*, 2664−2675.
(70) Riemenschneider, J.; Holzmann, J.; Ludwig, R. Salt Effects on the Structure of Water Probed by Attenuated Total Reflection Infrared Spectroscopy and Molecular Dynamics Simulations. *ChemPhysChem* **2008**, *9*, 2731−2736.
(71) Li, R. H.; Jiang, Z. P.; Guan, Y. T.; Yang, H. W.; Liu, B. Effects of Metal Ion on the Water Structure Studied by the Raman O-H Stretching Spectrum. *J. Raman Spectrosc.* **2009**, *40*, 1200−1204.
(72) Terpstra, P.; Combes, D.; Zwick, A. Effect of Salts on Dynamics of Water: A Raman Spectroscopy Study. *J. Chem. Phys.* **1990**, *92*, 65−70.
(73) Ishiyama, T.; Morita, A. Vibrational Spectroscopic Response of Intermolecular Orientational Correlation at the Water Surface. *J. Phys. Chem. C* **2009**, *113*, 16299−16302.
(74) Jarvis, N. L.; Scheiman, M. A. Surface Potentials of Aqueous Electrolyte Solutions. *J. Phys. Chem.* **1968**, *72*, 74−78.
(75) Randles, J. E. B. Structure at the Free Surface of Water and Aqueous Electrolyte Solutions. *Phys. Chem. Liq.* **1977**, *7*, 107−179.
(76) Verreault, D.; Allen, H. C. Bridging the Gap between Microscopic and Macroscopic Views of Air/Aqueous Salt Interfaces. *Chem. Phys. Lett.* **2013**, *586*, 1−9.
(77) Horinek, D.; Herz, A.; Vrbka, L.; Sedlmeier, F.; Mamatkulov, S. I.; Netz, R. R. Specific Ion Adsorption at the Air/Water Interface: The Role of Hydrophobic Solvation. *Chem. Phys. Lett.* **2009**, *479*, 173−183.
(78) Mähler, J.; Persson, I. A Study of the Hydration of the Alkali Metal Ions in Aqueous Solution. *Inorg. Chem.* **2012**, *51*, 425−438.